Colloid & Polymer Science Colloid Polym Sci 268:528–535 (1990)

Crystallization kinetics of isotactic polypropylene blended with atactic polystyrene

W. Wenig, H.-W. Fiedel and A. Scholl

Universität – GH – Duisburg, Laboratorium für Angewandte Physik, Duisburg, FRG

Abstract: Crystallization kinetic parameters, such as spherulitic growth rates, nucleation densities, and Avrami-exponents, have been determined by optical microscopy for isotactic polypropylene blended with atactic polystyrene. It is found that the crystallization of iPP is strongly influenced by the presence of polystyrene. With increasing PS concentration in the blend, the nucleation densities decrease, while the spherulitic growth rates as well as the positions of thermal peaks, measured by DSC, remain independent of sample composition. Due to the formation of interfaces as a consequence of increasing dispersion of polystyrene the nucleation changes from preferentially thermal to athermal.

Key words: Polypropylene/polystyrene blends, nucleation, isothermal crystallization, spherulitic growth

Introduction

According to most commonly employed criteria of miscibility of polymer blends, isotactic polypropylene and atactic polystyrene should be incompatible [1, 2]. Indeed, mixtures of both polymers show two glass transitions and the melting temperature of iPP/aPS is shifted only gradually as a function of the aPS content. However, it is found that the glass transition temperature shifts with blend composition and several investigations like mechanical and dilatometric measurements [3-5] lead some authors to the conclusion, that there is a special interaction between iPP and aPS [3, 5]. This interaction should influence the crystallization behavior of the crystallizable component. The aim of this paper is to investigate the crystallization kinetics of isotactic polypropylene in its blend with atactic polystyrene.

2.Experimental

2.1 Sample preparation

The polymers used for the blends were isotactic polypropylene with an average molecular weigth M_W = 468,000 and atactic polystyrene with M_w = 276,000. Appropriate amounts of both polymers (aPS weight fractions: 0 %...40 %; for thermal investigations 0 %...50 %) were dissolved in xylene followed by precipitation in an excess of methanol. The resulting powder was placed between the plates of a hydraulic press where it was heated to a temperature well above the melting temperature (ca. 220 °C) at a load of 10 kN. After switching off the heating of the press, the sample was allowed to cool to room temperature. The resulting thickness of the sample amounted to ca. 30 μm. Some thicker samples (d~80μm) have also been prepared to investigate the influence of the truncation effect.

2.2 Measurements

For observation in the optical microscope (Leitz Metallux II), the samples were placed between microscope slides and put in a Mettler hot-stage. Here they were heated to 483 K for 5 min. and then cooled to the chosen crystallization temperature T_c with an average cooling rate of 20 K/min. At a temperature of 2 K above the crystallization temperature, the cooling rate was lowered to 3 K/min to avoid cooling below T_c. Crossed polarizers were used and the crystallization was monitored on a video screen and recorded on tape. From the video recording, the growth of the spherulites and the nucleation density as a function of time were determined. The crystallization temperatures for isothermal crystallization were chosen between 402 K and 408 K with a temperature increment of 1 K. At lower crystallization temperatures, the crystallization proved to be too fast; at higher temperatures it appeared too slow. We consider this temperature range to be sufficient to investigate the influence of blend composition on the crystallization parameters. Each crystallization experiment was carried out five times at different locations of the sample to allow an error analysis. Findings showed that both the spherulitic growth

rate as well as the development of the number of nuclei as a function of time could be measured with great accuracy. DSC curves were recorded using a Perkin Elmer DSC II calorimeter. The heating rate was 20 K/min; the cooling rate 10 K/min. Wide-angle X-ray scattering curves were measured using a Philips PW 1380 goniometer. Cukα-radiation was used and monochromatisation was achieved by use of a graphite monochromator. The polypropylene crystallizes in all samples in the monoclinic α-modification, the hexagonal β-modification did not occur.

3. Results

3.1 Nucleation densities

Assuming a constant density M of nuclei, for isothermal crystallization the nuclei appear statistically with a probability v of developing per unit time [6–13]

$$N(t) = vMe^{-vt} \tag{1}$$

where $N(t)$ is the nucleation frequency per unit of untransformed volume at time t. Integration of Eq. (1) yields the number of nuclei as a function of time:

$$N(t) = M(1 - e^{-vt}). \tag{2}$$

Figure 1 shows $N(t)$ for the sample containing 20 % aPS. Using Eq. (2), the nucleation density M and the probability v can be determined. These values are listed in Tables 1 and 2.

Assuming that at a given temperature the number of nucleating sites is distributed normally as a function of temperature, the equation obtained for the temperature dependence of the nucleation density [8] is

$$M(T) = M_0 \frac{1}{\sigma\sqrt{2\pi}} \int_T^\infty e^{-[(x-\bar{T})^2/(2\sigma^2)]} dx \tag{3}$$

Table 1. Nucleation densities

Crystallization temperature		$M/10^3$ mm^{-3}			
T_c /K	$c_{iPP} = 1$	0.9	0.8	0.7	0.6
408	0.4	3.5	4.3	2.5	2.7
407	0.7	3.2	5.1	2.5	4.3
406	1.1	3.4	3.7	2.6	2.0
405	1.5	3.7	3.6	2.8	1.8
404	1.7	3.3	3.7	2.7	2.4
403	2.6	3.8	3.9	2.9	2.4
402	2.1	3.9	4.3	3.4	2.5

Table 2. Nucleus activation frequency

Crystallization temperature		$v/10^2$			
T_c /K	$c_{iPP} = 1$	0.9	0.8	0.7	0.6
408	2.4	2.0	0.4	0.4	0.3
407	0.6	1.5	0.5	0.6	0.2
406	1.7	1.5	1.0	0.8	0.5
405	1.6	0.6	1.5	0.6	0.4
404	1.5	0.8	1.9	1.3	1.7
403	2.8	0.7	2.6	8.0	3.2
402	4.9	0.2	3.7	1.4	2.2

where M_0 = total nucleation density; σ = standard deviation of the distribution, and $\bar{T}$ = temperature of the distribution maximum. M_0 can be determined from the experiment using Eq. (3) by a numerical method (Newtonian approximation). The results are listed in Table 3. Figure 2 shows $M(T)$ for polypropylene.

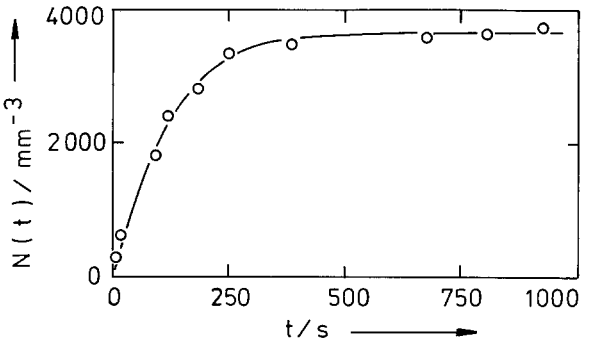

Fig. 1. Number of nuclei as a function of time for a sample containing 20% aPS (T_c = 406 K, M = 3.7 10^3 /mm^{-3}, $v = 10^{-2}$).

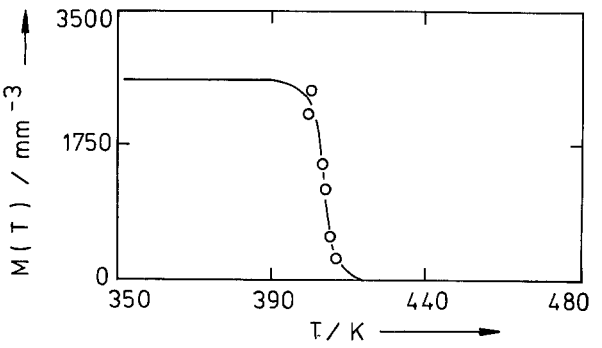

Fig. 2. Temperature dependence of the nucleation density for polypropylene

Table 3. Total nucleation density and standard deviation of the distribution of nucleating sites (variance)

Polypropylene weight fraction c_{iPP}	Total nucleation density $M_0/10^3$ mm^{-3}	Variance σ/K^{-1}
1	2.7	2.6
0.9	6.7	25.9
0.8	7.2	18.7
0.7	5.3	25.3
0.6	4.0	9.9

3.2 *Spherulitic growth rates*

For the system investigated, the growth rate of a spherulite is defined by

$$G = \frac{\Delta r}{\Delta t} \tag{4}$$

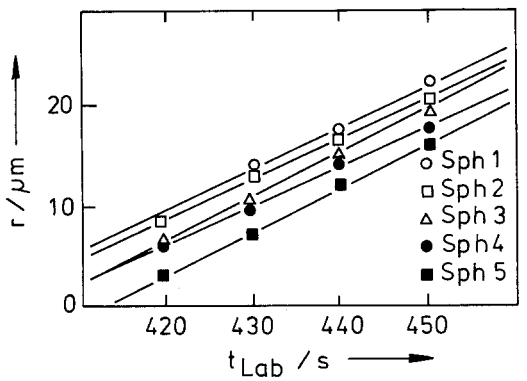

Fig. 3. Radii of five observed spherulites as a function of time for polypropylene (T_c = 406 K)

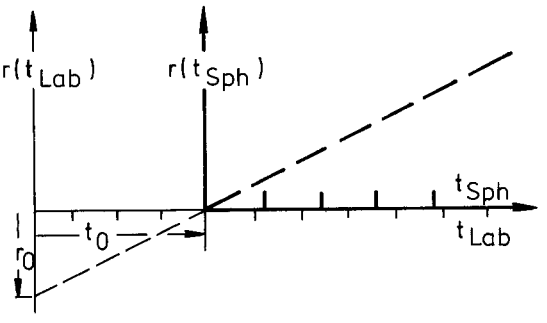

Fig. 4. Shift of the coordinate system for the spherulitic radius to determine the initial time for the spherulitic growth

where r is the spherulitic radius. The initial time for the spherulitic growth can be determined as follows: The radius of the i-th spherulite as a function of the observation time t_{Lab} is given by

$$r_i(t_{Lab}) = G_i\, t_{Lab} + r_{o,\,i} \tag{5}$$

where $r_{o,i}$ is the radius of the i-th spherulite at $t_{\mathrm{Lab}} = 0$. Because the spherulites are nucleated at different times, any experiment yields a distribution of the spherulitic radii. Figure 3 displays the development of the spherulitic radius of five observed spherulites as a function of t_{Lab}. The arithmetic average of the slopes of the straight lines

$$G_m = \frac{1}{k} \sum_{i=1}^{k} \frac{\Delta r_i}{\Delta t_i} \tag{6}$$

already yields a good approximation of the average growth rate. The initial time of the growth curves is then determined by linear regression of the functions r_i (t_{Lab}) and introducing the time variable t_{Sph} which follows the condition r (t_{Sph} = 0) = 0. This transformation is displayed in Fig. 4. From this figure we take

$$t_{Lab} = t_{Sph} + t_o. \tag{7}$$

With Eq. (5) we obtain

$$r_i(t) = G_i \cdot (t_{Sph} + t_{o,i}) + r_{o,i} \tag{8}$$

$$r_{o,i} = G \cdot (-t_o) = -G_o t_o. \tag{8a}$$

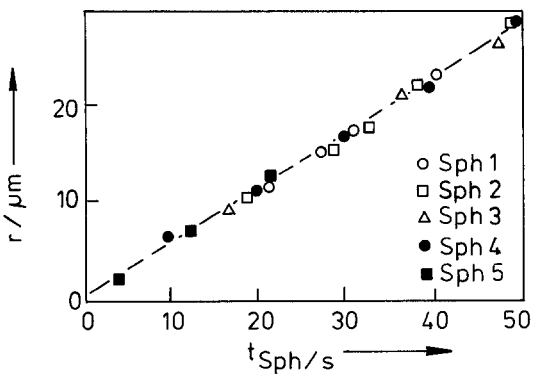

Fig. 5. Radii of five observed spherulites as a function of time after correction for initial time (T_c = 406 K)

For r_i as a function of time we now obtain

$$r_i(t_{Sph,i}) = G_i\, t_{Sph,i} \tag{9}$$

and for the average growth function

$$r(t_{Sph}) = G_m t_{Sph} + r_o. \tag{10}$$

Figure 5 shows, as an example, the radii of five observed spherulites as a function of t_{Sph} for polypropylene. The experimentally determined values for the growth rates are listed in Table 4.

Table 4. Spherulitic growth rates

Crystallization temperature	$G/10^{-4}$ mm s^{-1}				
T_c/K	$c_{iPP} = 1$	0.9	0.8	0.7	0.6
408	0.29	0.14	0.28	0.31	0.24
407	0.41	0.25	0.33	0.37	0.24
406	0.53	0.27	0.52	0.47	0.35
405	0.43	0.30	0.58	0.55	0.49
404	0.73	0.29	0.67	0.64	0.50
403	1.02	0.52	0.95	0.91	0.62
402	1.12	0.40	1.03	1.41	0.64

Within the investigated range of crystallization temperatures, only one regime of lamellar growth can be expected (Regime III) and the spherulitic growth rate increases exponentially with the supercooling. This temperature dependence can be calculated from [16–18]

$$G(T) = \begin{cases} 0; & (T \le T_g - C_2) \\ G_0 e^{-C_1C_2/(C_2+T-T_g)} e^{-C_3/[T(T_m^0 - T)]}; & (T_g - C_2 < T < T_m^o) \\ 0; & (T \ge T_m^o) \end{cases} \tag{11}$$

where T_g = glass temperature, T_m° = melting temperature, and G_o, C_1, C_2, C_3 = parameters describing the growth rate behavior [8].

For polypropylene, C_1 and C_2 can be taken from the literature [8] ($C_1 = 25$, $C_2 = 30$ K). T_g and T_m° can be measured. G_o and C_3, which is strongly dependent on the melting temperature T_m°, can be obtained from a plot of $\ln G + C_1C_2 / (C_2 + T - T_g)$ versus $1/[T(T_m^\circ - T)]$. Figure 6 shows such a plot for polypropylene. The values for G_o and C_3 are listed in Table 5. Using these values, the function $G(T)$ can be calculated (Fig. 7).

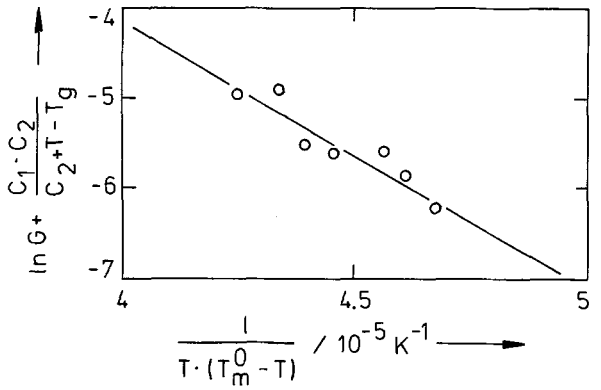

Fig. 6. Plot to determine the parameters G_o and C_3. ($C_1 = 25$, $C_2 = 30$ K, $T_g = 260$ K, $T_m^\circ = 460.5$K)

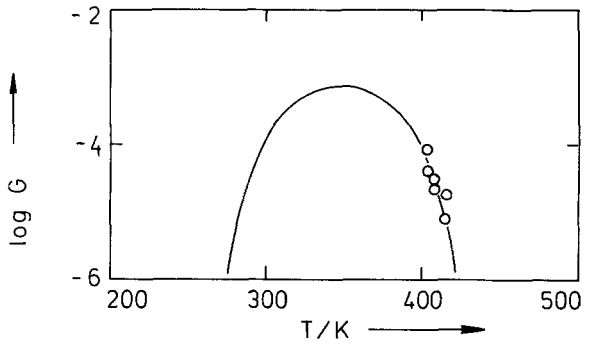

Fig. 7. Temperature dependence of the spherulitic growth rate for polypropylene [experimental values were fitted using the function defined in Eq. (11)]

Table 5. Parameters G_o and C_3 to determine the temperature dependence of the spherulitic growth rates ($C_1 = 25$, $C_2 = 30$ K, $T_g = 260$ K, $T_m^o = 460.5$K)

Polypropylene weight fraction	$G_o/10^{-3}$ mm s^{-1}	$C_3/10^{-5}$ K^2
c_{iPP}		
1.0	1.1	2.8
0.9	0.6	2.8
0.8	38.3	3.6
0.7	69.5	3.7
0.6	2.6	3.1

3.3 *Avrami-exponents*

The development of the crystallinity as a function of time in a crystallizing polymer can be described by the Avrami-equation [14, 15]:

$$1 - X^c = e^{-kt^n} \tag{12}$$

where X^c = fraction of transformed (spherulitic) material, k = characteristic constant, and n = 'Avrami-exponent' describing the kind of crystallization; and

$$X^c = \frac{v^c}{v_m^c} \tag{13}$$

where v^c = volume crystallinity, v_m^c = crystallinity after complete crystallization.

Exponents k and n can be determined by plotting the crystallinity versus time. Using the equation

$$\log [-\ln(1 - X^c)] = \log k + n \log t, \tag{14}$$

k and n are yielded by plotting log [-ln (1 - X^c)] versus log t. Figure 8 shows such a plot for polypropylene. The values for k and n are listed in Table 6.

Table 6. Avrami-exponents and constants (T_c = 408 K)

Polypropylene weight fraction c_{iPP}	n	k
1.0	2.7	$1.7\ 10^{-10}$
0.9	2.6	$1.3\ 10^{-13}$
0.8	2.3	$2.2\ 10^{-8}$
0.7	2.4	$9.5\ 10^{-9}$
0.6	1.7	$7.8\ 10^{-7}$

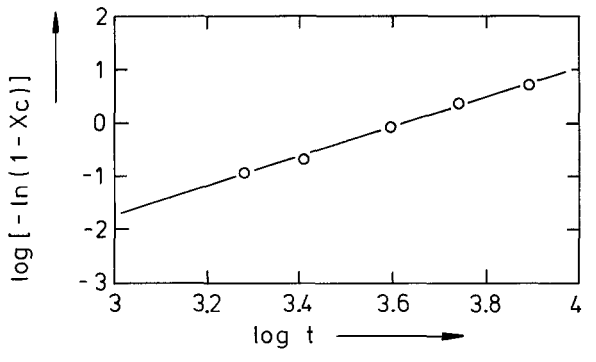

Fig. 8. Plot to determine the Avrami-exponent (polypropylene, T_c = 408 K)

4. Discussion

Specific interactions between iPP and PS have been concluded from DTA, dilatometric measurements and mechanical analysis. Han et al. [3] finds a higher degree of dispersion of the two components in extruded blends, which was concluded from a correlation between blend composition and thermal spectra area of DTA curves. Mucha [5] observes a decrease of the melting temperature of iPP with increasing PS weight fraction accompanied by a linear decrease of the area under the thermal spectra. From the decrease of T_m as a function of aPS-concentration, a nucleation effect at the interfaces is concluded.

In Fig. 9, the DSC curves of the investigated samples are displayed. No shift of the melting

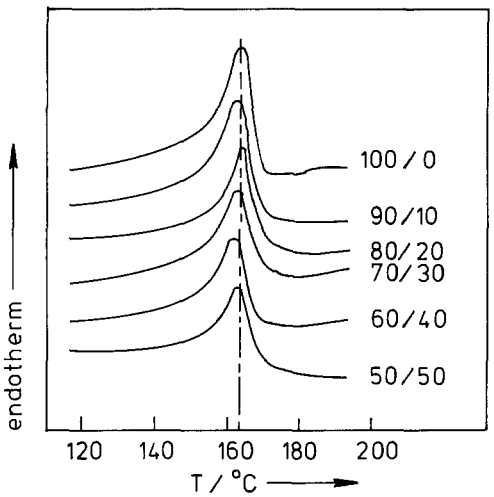

Fig. 9. DSC curves of the investigated samples

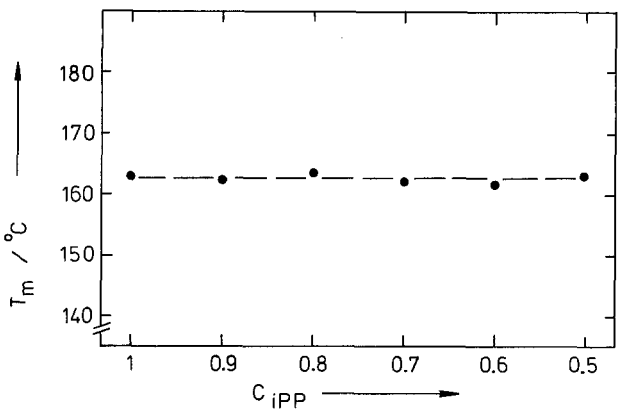

Fig. 10. Melting temperatures versus polypropylene concentration

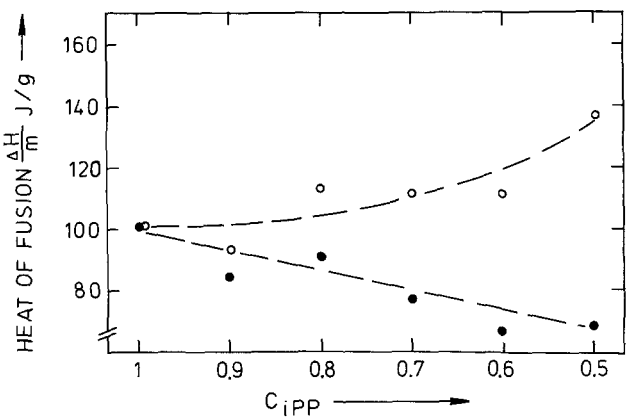

Fig. 11. Heats of fusion of the investigated blends (●) and of the PP component (○)

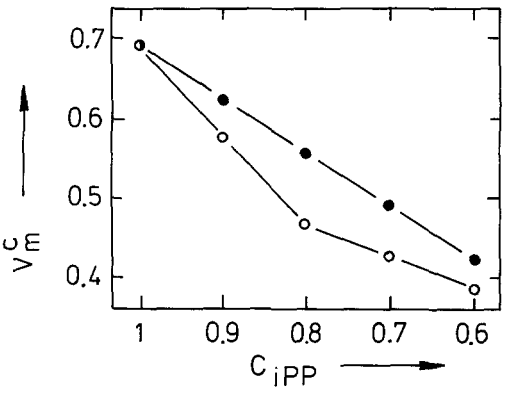

Fig. 12. Crystallinity after complete crystallization (T_c = 407 K) as a function of iPP weight fraction [○ = measured crystallinity (WAXS), ● = decrease of the crystallinity that can be expected from the dilution effect]

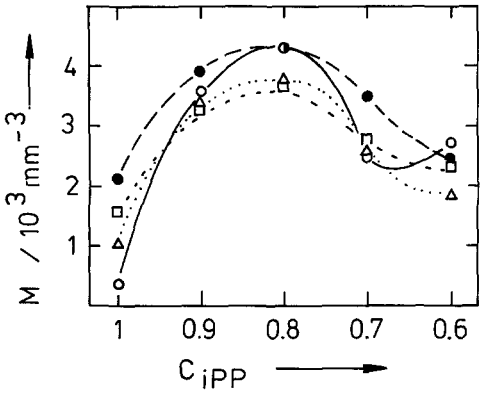

Fig. 13. Nucelation density as a function of polypropylene weight fraction
(●: T_c = 402 K, △: T_c = 404 K, △: T_c = 406 K, ○: T_c = 408 K)

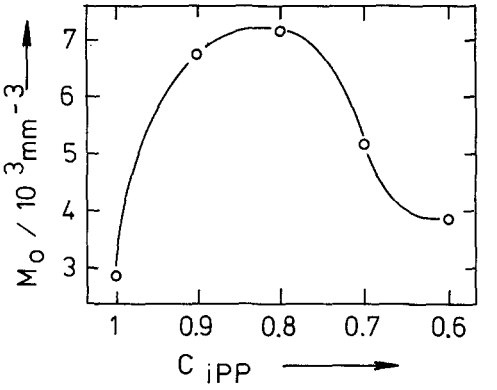

Fig. 14. Total nucleation density as a function of polypropylene weight fraction

temperature is observed (cf. Fig. 10). The heats of fusion (Fig. 11) decrease with the iPP-concentration. The values of $\Delta H/m$ for the iPP component are also plotted in Fig. 11. We see a slightly increasing curve, which means that the aPP cannot be dispersed in the blend to such an extent that it effects the melting properties of the polypropylene component. Therefore, we expect the crystallinity to drop linearly with composition as a consequence of the dilution of the crystallizable component.

As Fig. 12 reveals, we find a steeper decrease of v_m^c than can be expected from the dilution of the iPP fraction by the PS component. The difference between the measured from the expected values is maximal at c_{iPP} = 0.8, while for higher PS concentrations the values converge. This indicates a concentration dependent interaction of the two components and we expect to find an effect on the crystallization parameters at this particular composition.

Figure 13 shows the nucleation density as a function of sample composition. We observe that M increases with decreasing iPP content and surpasses a maximum at c_{iPP} = 0.8. At lower iPP concentrations M decreases, but seems to increase again for $c_{iPP} < 0.6$. This could be the result of dispersion of polystyrene in polypropylene. With increasing PS concentration, polypropylene/polystyrene interfaces are created at which surface nucleation may occur. The decrease of the nucleation density for PS-concentrations >20 % may then be a result of an agglomeration of PS domains causing the surface area of the PS component to decrease. At higher PS-concentrations, the surface area increases again causing the nucleation density to increase.

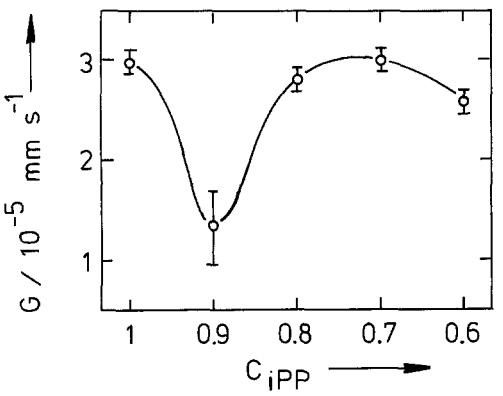

Fig. 15. Spherulitic growth rate as a function of polypropylene weight fraction (T_c = 408 K)

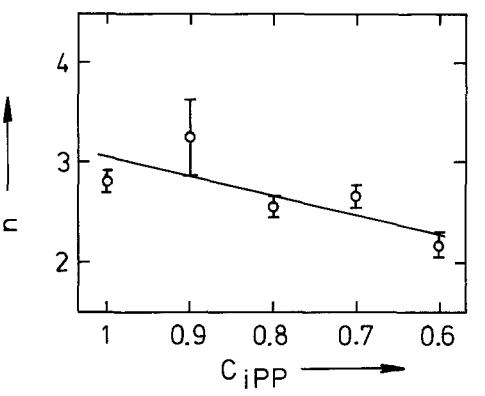

Fig. 16. Avrami-exponent n as a function of polypropylene weight fraction (T_c = 408 K)

For all blends and at all crystallization temperatures we find the nucleation density higher than in polypropylene. Also, the total nucleation density, which is plotted in Fig. 14, shows this behavior. Obviously, additional nucleation at the PS surfaces contributes to the overall nucleation density.

The spherulitic growth rate, displayed in Fig. 15, seems to be independent of sample composition: it is constant within the experimental error except for the value at c_{iPP} = 0.9, where G is lower. This value, however, is connected with a larger experimental error, so that it is difficult to conclude a possible hindrance of the spherulitic growth at this particular PS-concentration. A second sample, prepared the same way, showed a similar behavior. Possibly, the dispersion of the PS in the polypropylene was not homogeneous with this composition. This, however, is difficult to investigate under the microscope.

Further insight into the crystallization behavior, especially into the type of nucleation, is provided by the Avrami-exponent n. In Fig. 16, n is plotted for T_c = 408 K. We observe that n assumes values between 2 and 3 and decreases with increasing PS-concentration. For unhindered three-dimensional growth, we should expect Avrami-exponents between 3 (athermal nucleation) and 4 (thermal nucleation) [19]. Deviations from these values may be due to truncations of the spherulites [20–22], which in this case should reduce the Avrami-exponent. Obviously, this situation applies here and we have, at least in part, two-dimensional growth of the PP spherulites. The value n = 3 for polypropylene then means that the nucleation is preferentially thermal. With increasing PS content the Avrami-exponent decreases and the nucleation becomes athermal. This can only be the effect of surface nucleation (heterogeneous nucleation) at the PS interfaces. Due to constant thickness of the samples, the truncation effect should be constant.

It is, however, possible that the calculated Avrami-exponent is a complex combination of volume limitation and surface nucleation. Of importance would then be the truncations of the spherulites due to the existence of interfaces, which would reduce the Avrami-exponent proportional to the PS-concentration and the dispersion of the polystyrene in the polypropylene melt. We found, however, that the PS domains are incorporated into the PP spherulites during their growth. Also, there is no indication that the spherulitic growth rate is influenced by the dispersed polystyrene.

From this discussion we draw the following conclusions:

1. The crystallization kinetics of isotactic polypropylene in its blend with atactic polystyrene is strongly dependent on blend composition.
2. Polystyrene is, proportional to its concentration in the blend, increasingly dispersed and creates interfaces.
3. Due to the formation of interfaces, the nucleation changes from preferentially thermal to athermal.
4. The blending of polystyrene to polypropylene does not affect the growth rates of the polypropylene spherulites.

Acknowledgement:

The authors are grateful to A. Wasiak for many helpful discussions.

References

1. Krause S (1972) J Macromol Sci — Rev Macromol Chem C7:251
2. Paul DR, Newman S (1978) Polymer Blends. Academic Press, New York
3. Han CD, Villamizar CA, Kim YW, Chen SJ (1977) J Appl Polym Sci 21:353
4. Krasnikova NP, Kotova EV, Vinogradov GV, Pelzbauer Z (1978) J Appl Polym Sci 22:2081
5. Mucha M (1986) Coll & Polymer Sci 264:859
6. Mandelkern L (1963) Crystallization of Polymers. Mc Graw Hill, New York
7. Wunderlich B (1973) Macromolecular Physics. Academic Press, New York
8. Icenogle RD (1985) J Polym Sci Phys Ed 23:1369
9. Hoshino S, Powers J, Stein RS (1962) ONR Technical Report No 43
10. Hoshino S, Meinecke E, Powers J, Stein RS (1965) J Polym Sci A-2 3:3041
11. Boon J, Challa G, van Krevelen DW (1968) J Polym Sci A-2 6:1791
12. Boon J, Challa G, van Krevelen DW (1968) J Polym Sci A-2 6:1835
13. Wang TT, Nishi T (1977) Macromolecules 10:421
14. Avrami M (1941) J Chem Phys 9:177
15. Mandelkern L (1958) Growth and Perfection of Crystals. John Wiley & Sons, New York
16. Hoffmann JD, Frolen LJ, Ross GS, Lauritzen JI (1975) J Res Natl Bur Stand 79A:671
17. Hoffmann JD (1983) Polymer 24:3
18. Suzuki T, Kovacs A (1970) Polymer J 1:82
19. Binsbergen FL, DeLange BGM (1970) Polymer 11:309
20. Escleine JM, Monasse B, Wey E, Haudin JM (1984) Colloid Polym Sci 262:366
21. Monasse B, Haudin JM (1985) Colloid Polym Sci 263:822
22. Billon N, Escleine JM, Haudin JM (1989) Colloid Polym Sci 267:668

Received June 6, 1989
accepted October 27, 1989

Author's address:
W. Wenig
Universität – GH – Duisburg
Laboratorium für Angewandte Physik
Lotharstr. 1
4100 Duisburg, FRG